

1 Stratospheric eruptions from tropical and extra-tropical volcanoes constrained  
2 using high-resolution sulfur isotopes in ice cores

3

4 Andrea Burke<sup>1,2</sup>, Kathryn A. Moore<sup>1,3</sup>, Michael Sigl<sup>4,5</sup>, Dan C. Nita<sup>1,6</sup>, Joseph R.  
5 McConnell<sup>5</sup>, and Jess F. Adkins<sup>2</sup>

6

7 <sup>1</sup>School of Earth and Environmental Sciences, University of St Andrews, UK

8 <sup>2</sup>Division of Geological and Planetary Sciences, Caltech, USA

9 <sup>3</sup>Department of Atmospheric Science, Colorado State University, USA

10 <sup>4</sup>Climate and Environmental Physics, University of Bern, Switzerland

11 <sup>5</sup>Division of Hydrologic Sciences, Desert Research Institute, USA

12 <sup>6</sup> Department of Geology, Babes-Bolyai University, Romania

13

## 14 **Abstract**

15 The record of volcanic forcing of climate over the past 2500 years is based  
16 primarily on sulfate concentrations in ice cores. Of particular interest are large  
17 volcanic eruptions with plumes that reached high altitudes in the stratosphere,  
18 as these afford sulfate aerosols the longest residence time in the atmosphere, and  
19 thus have the greatest impact on radiative forcing. Sulfur isotopes measured in  
20 ice cores can be used to identify these large eruptions because stratospheric  
21 sulfur is exposed to UV radiation, which imparts a time-evolving mass  
22 independent fractionation (MIF) that is preserved in the ice. However sample  
23 size requirements of traditional measurement techniques mean that the MIF  
24 signal may be obscured, leading to an inconclusive result. Here we present a new  
25 method of measuring sulfur isotopes in ice cores by multi-collector inductively

coupled plasma mass spectrometry, which reduces sample size requirements by three orders of magnitude. Our method allows us to measure samples containing as little as 10 nmol of sulfur, with a precision of 0.11‰ for  $\delta^{34}\text{S}$  and 0.10‰ for  $\Delta^{33}\text{S}$ , enabling a high-temporal resolution over ice core sulfate peaks. We tested this method on known tropical (Tambora 1815 and Samalas 1257) and extra-tropical (Katmai/Novarupta 1912) stratospheric eruptions from the Tunu2013 ice core in Greenland and the B40 ice core from Antarctica. These high-resolution sulfur isotope records suggest a distinct difference between the signatures of tropical versus extra-tropical eruptions. Furthermore, isotope mass balance on extra-tropical eruptions provides a means to estimate the fraction of sulfate deposited that was derived from the stratosphere. This technique applied to unidentified eruptions in ice cores may thus improve the record of explosive volcanism and its forcing of climate.

**Keywords:** volcanoes, sulfur, mass-independent fractionation, stratosphere, Katmai, ice cores

## 1 Introduction

Volcanic eruptions are the main natural external forcing of climate over the past millennium (Schurer, 2013). The  $\text{SO}_2$  erupted from volcanoes is oxidized to sulfate in the atmosphere, and these sulfate aerosols reflect incoming radiation, and cool the planet. The largest climatic impacts occur when volcanic eruption columns reach high altitudes in the stratosphere, as the aerosols remain in the atmosphere for longer, with a residence time of a couple of years (Robock,

2000). In contrast, sulfate aerosols that are erupted into the troposphere are efficiently removed on the order of weeks. Accurate reconstruction of climate forcing by large volcanic eruptions is fundamental for deconvolving forced from internal climate variability and for better understanding climate sensitivity to greenhouse gases.

Current state-of-the art volcanic forcing records are based on sulfate concentrations in ice cores, which show peaks above background levels due to volcanic eruptions (e.g. Gao et al., 2007; Sigl et al., 2015). Sulfate concentrations from several cores are spatially averaged to determine the total mass deposition rate (i.e. “flux”) of sulfate to the ice sheet for a given eruption, and this is then scaled to a total stratospheric burden of sulfate, which can be used to calculate radiative forcing changes or aerosol optical depth fields (e.g. Toohey and Sigl, 2017). However, sulfate concentrations in ice can also be elevated due to local, smaller eruptions that did not make it to high altitudes in the stratosphere and thus would not have had a large climatic impact. To address this complication, ice core sulfate records from Greenland and Antarctica have been synchronized and compared to determine which sulfate peaks occur in both hemispheres. These peaks are called ‘bipolar events’, and are attributed to large, tropical eruptions whose plumes made it to the stratosphere and thus were distributed globally, allowing for deposition of sulfate aerosols in both hemispheres (e.g. Plummer et al., 2012; Sigl et al., 2013). These events are then scaled to have a larger effect on the radiative forcing of climate compared to sulfate events that occur in only one of hemispheres (Gao et al., 2008; Sigl et al., 2015; Toohey and Sigl, 2017). However, this approach is not without its difficulties: the attribution of a bipolar event relies on very precise ice core age models, and typical age

uncertainties over the past two thousand years can be of the order of 2-4 years (McConnell et al., 2018; Sigl et al., 2015). Thus, based on sulfate concentration alone it is not possible to distinguish between a bipolar event, and two hemispheric events that occur within age model uncertainty of each other. For mid-to-high latitude eruptions (producing unipolar sulfate signals), it is also not possible to determine how much of the sulfate deposited on the ice sheet came via the stratosphere since a large proportion could be transported tropospherically. Given the large difference in the radiative forcing following eruptions with high stratospheric injection height (i.e. 24 km or higher) compared to eruptions with lower injection heights (Toohey et al., 2019), there is a need for a means to independently constrain volcanic sulfate injections to the high stratosphere.

Sulfur isotopes have been used in polar snow (Baroni et al., 2007) and ice cores (e.g. Baroni et al., 2008; Cole-Dai et al., 2009; Gautier et al., 2019; Savarino, 2003) to distinguish between eruptions whose plumes reached the stratosphere at or above the ozone layer and those that remained below. This approach is possible because the sulfur that makes it up to the ozone layer is exposed to UV radiation, which imparts a mass independent fractionation (MIF) of the S isotopes (Farquhar et al., 2001). This fractionation is then recorded in the ice cores as a non-zero  $\Delta^{33}\text{S}$  value, where

$$\Delta^{33}\text{S} (\text{‰}) = \delta^{33}\text{S} - ((\delta^{34}\text{S} + 1)^{0.515} - 1) \text{ (Equation 1)}$$

and  $\delta^{33}\text{S} = (^{33}\text{S}/^{32}\text{S})_{\text{sample}} / (^{33}\text{S}/^{32}\text{S})_{\text{reference}} - 1$ , with x either 33 or 34. Almost all physical, chemical and biological processes fractionate isotopes based on mass, and thus have  $\Delta^{33}\text{S}$  values that are zero. Sulfur photochemistry is one of the few processes that produces mass-independent fractionation, even though the exact

photochemical mechanism for this fractionation is still debated (e.g. Gautier et al., 2018). The presence of non-zero  $\Delta^{33}\text{S}$  in sulfate in ice therefore indicates that the sulfate formation occurred at a height in the stratosphere where it is possible to interact with UV radiation. Although sulfur isotopes have previously been used as a means to distinguish between stratospheric and tropospheric eruptions (e.g. Lanciki et al., 2012), an important caveat is that at high latitudes, the lower stratosphere lies below the ozone layer (Fig. 1), and so it is possible to have a high latitude eruption that reaches the lower stratosphere that does not result in a MIF signature in polar ice (Schmidt et al., 2012). However, recent modelling work (Toohey et al., 2019) shows that high latitude eruptions that only penetrate into the upper troposphere/lower stratosphere (UT/LS) have reduced radiative forcings because of shorter sulfate aerosol residence times. The unambiguous identification of volcanic events that had plumes that reached altitudes in the stratosphere at or above the ozone layer, and thus had long atmospheric residence times, would represent a major improvement of the record of volcanic forcing of climate.

Sulfur isotopes are traditionally measured by gas-source mass spectrometry. These methods require a micromole of sulfur for analysis and thus entire sulfate peaks were analyzed from a single ice core (Baroni et al., 2008) or multiple ice cores were synchronized and combined (Gautier et al., 2019; 2018) to get enough sulfate from an individual eruption. Since the  $\Delta^{33}\text{S}$  signature is time-evolving from positive to negative over the course of the sulfate deposition on the ice sheet (Baroni et al., 2007), the integration over an entire peak may give  $\Delta^{33}\text{S} = 0$  (Baroni et al., 2008), resulting in ambiguity in the fingerprinting of stratospheric eruptions. To resolve this issue we applied a new

technique of S isotope measurement by MC-ICP-MS to ice cores (McConnell et al., 2017; Paris et al., 2013). This method requires only 10 nmol of sulfate, allowing up to bi-monthly resolution. We applied this technique to two known tropical stratospheric eruptions (Tambora 1815 and Samalas 1257), as well as a known high latitude stratospheric eruption (Katmai/Novarupta 1912) to test the applicability of this approach for volcanic eruptions proximal to the ice sheet.

## **2 Methods**

Ice core samples were collected from the Tunu2013 core from Greenland (78° 2.1' N 33° 52.8' W, 2105 m; 213 m deep; collected May 2013 (Sigl et al., 2015)) for three large volcanic eruptions: the 1815 eruption of Tambora (Indonesia), the 1257 eruption of Samalas (Indonesia), and the 1912 eruption of Katmai/Novarupta, henceforth Katmai (Alaska, US). The eruption of Samalas was also replicated from the B40 core from Antarctica (75° 0' S 0° 4.1' E, 2890 m; 200 m deep; collected December 2012 (Sigl et al., 2014)). The age models and continuous sulfur concentration measurements from these ice cores (Sigl et al., 2015) were used to identify the volcanic peaks. Samples were cut from the wings of cores at a resolution of ~2-3 cm over the course of each volcanic event and a resolution of 5 cm for background analyses pre- and post-event. Each sample was measured twice, so a total of 20 nmol was used (only 4 mL for event samples (5 uM) to 40 mL for background samples (0.5 uM)), making this method preferable for high-resolution work on precious sample material. Outside edges of the ice core were scraped clean and the samples were melted. Sulfate concentration was determined by ion chromatography on a 500 µL aliquot.

151 These concentrations (circles, Fig 2 a,b, Fig 3 a) were compared to continuous  
152 sulfur measurements (Sigl et al., 2015) to validate which part of the peak was  
153 sampled in the discrete samples, and to determine the amount of sample needed  
154 for two isotope measurements (20 nmol total). The appropriate amount of  
155 sample was then dried down and redissolved in 70  $\mu$ L of 0.01% v/v distilled HCl  
156 under clean laboratory conditions. The samples were passed through Teflon  
157 columns made from 4:1 PTFE heat shrink tubing (11 mm expanded diameter)  
158 that were loaded with 35  $\mu$ l of clean AG1X8 anion-exchange resin in order to  
159 separate out the sulfate from the sample matrix. Prior to sample loading, the  
160 resin was cleaned with 350  $\mu$ l of 1.6 M HNO<sub>3</sub>, 350  $\mu$ l of 1.2 M HCl, and 350  $\mu$ l of  
161 0.6 M HCl. Samples were then loaded and cations were removed by rinsing the  
162 column with 3 times 175  $\mu$ l of MilliQ water, followed by sulfate elution in 3 $\times$ 70  $\mu$ l  
163 of 0.5 M HNO<sub>3</sub>. The eluted samples were evaporated to dryness, resuspended in  
164 0.5 M HNO<sub>3</sub>, and NaOH was added to the sample to match the concentration and  
165 matrix of the in-house Na<sub>2</sub>SO<sub>4</sub> bracketing standard (Paris et al., 2013).

166 Triple sulfur isotopes (<sup>32</sup>S, <sup>33</sup>S, <sup>34</sup>S)<sup>1</sup> were measured by MC-ICP-MS using  
167 sample-standard bracketing with an in-house Na<sub>2</sub>SO<sub>4</sub> standard (Paris et al.,  
168 2013) at both Caltech and the STAiG lab at the University of St Andrews, and are  
169 reported relative to Vienna-Canyon Diablo Troilite (V-CDT). Each sample was  
170 measured at least twice. Long-term external reproducibility on the Caltech  
171 Switzer Falls secondary river water standard (Burke et al., 2018) was  $\delta^{34}\text{S} =$   
172  $4.11 \pm 0.24$  and  $\Delta^{33}\text{S} = 0.05 \pm 0.18$  ‰ (2 s.d., n = 10) at Caltech and  $\delta^{34}\text{S} = 4.17 \pm$

---

<sup>1</sup> Although <sup>36</sup>S provides further information about the oxidation process in the atmosphere (Gautier et al., 2018), it is not possible to measure <sup>36</sup>S by MC-ICP-MS because the argon plasma results in an interference from <sup>36</sup>Ar.

0.11 and  $\Delta^{33}\text{S} = 0.01 \pm 0.10 \text{ ‰}$  (2 s.d., n = 16) at St Andrews (Supplemental Data Table 3). Procedural blanks were run with each set of columns at Caltech and St Andrews, and the values were  $0.12 \pm 0.02 \text{ nmol}$  with a  $\delta^{34}\text{S}$  value of  $-0.2 \pm 2.8 \text{ ‰}$  (2 s.d., n = 3) for Caltech and  $0.14 \pm 0.04 \text{ nmol}$  with a  $\delta^{34}\text{S}$  value of  $5.5 \pm 1.9 \text{ ‰}$  (2 s.d., n = 9) for St Andrews (Supplemental Data Table 4). All reported  $\delta^{34}\text{S}$  and  $\delta^{33}\text{S}$  values were blank corrected with the long-term blank averages, and errors were propagated.  $\Delta^{33}\text{S}$  values were calculated following Equation 1.

Background ice core samples were measured prior to the volcanic sulfate events. These background samples were used to correct the measured sulfate isotope values ( $\delta_{\text{meas}}$ ) for background sulfate to determine the isotope values of the volcanic sulfate ( $\delta_{\text{volc}}$ ) following equation 2 (Baroni et al., 2007) :

$$\delta_{\text{volc}} = (\delta_{\text{meas}} - f_{\text{bkgd}}\delta_{\text{bkgd}})/f_{\text{volc}} \quad (\text{Equation 2})$$

where  $\delta_{\text{bkgd}}$  is the  $\delta^{34}\text{S}$  or  $\delta^{33}\text{S}$  of the background sample,  $f_{\text{bkgd}}$  is the mass fraction of the total sulfate that can be attributed to the background ( $f_{\text{bkgd}} = [\text{SO}_4]_{\text{bkgd}}/[\text{SO}_4]_{\text{sample}}$ ), and  $f_{\text{volc}}$  is the mass fraction of the total sulfate that can be attributed to volcanic sulfate ( $f_{\text{volc}} = 1 - f_{\text{bkgd}}$ ). Following Gautier et al. (2018) we only plotted those samples with more than 65% volcanic sulfate ( $f_{\text{volc}} > 0.65$ ).

### 3 Results

Each of the three volcanic events show non-zero  $\Delta^{33}\text{S}$  (Figs 2 and 3, Supplementary Data Table 1), with an evolution from positive to negative over the course of the sulfate deposition (Baroni et al., 2007), and there is good



agreement (Fig 4) between the records of the Samalas eruption in Greenland (Tunu2013) and Antarctica (B40). In the Tunu2013 core, the magnitude of the  $\Delta^{33}\text{S}$  is larger for sulfate associated with the Samalas and Tambora eruptions (1.9‰ and 1.7‰, respectively; Fig 2) than it is for the Katmai eruption, which only has a magnitude of 0.4‰ (Fig 3). The lowest  $\Delta^{33}\text{S}$  values for the Samalas and Tambora eruptions are negative (-1.8 and -0.8 ‰), whereas the lowest  $\Delta^{33}\text{S}$  values for the Katmai eruptions are within uncertainty of 0‰. In B40, the  $\Delta^{33}\text{S}$  values for Samalas range from 1.4 to -1.5‰.

In the two tropical eruptions (Fig 2),  $\delta^{34}\text{S}$  follows the same shape as the  $\Delta^{33}\text{S}$ , with an initial increase to 27.5‰ for Samalas and 20.6‰ for Tambora, dropping to -19.1‰ and -5.9‰ respectively over the course of the deposition of the sulfate. In contrast, for the Katmai eruption the  $\delta^{34}\text{S}$  initially decreases from its background value of 7.2‰ down to 0.6‰, before increasing back up to 4.6‰ (Fig 3). In B40, the  $\delta^{34}\text{S}$  values for Samalas range from 17.3 to -12.5‰ (Supplementary Data Table 1).

Pre-event background samples were measured for both the Samalas and Katmai eruptions.  $\delta^{34}\text{S}$  values prior to the Samalas event in Tunu2013 ranged from 9.1 to 11.1 ‰ with an average concentration of 0.4  $\mu\text{M}$ , and prior to the Katmai event were 7.2 ‰ at a concentration of 1.3  $\mu\text{M}$ . The  $\delta^{34}\text{S}$  value prior to the Samalas event in B40 was 13.9‰ at a concentration of 0.6  $\mu\text{M}$ . All background samples had  $\Delta^{33}\text{S}$  values within uncertainty of 0‰. Although we attempted to measure a pre-event background for Tambora, the sample that was cut from the ice core included the onset of the volcanic sulfate peak, and had a  $\Delta^{33}\text{S}$  value of 0.5‰. Thus, the average of 13 non-volcanic pre-industrial

background samples from other intervals of the Tunu2013 ice core ( $\delta^{34}\text{S} = 9.2 \pm 0.93\text{‰}$ ,  $\Delta^{33}\text{S} = 0.03 \pm 0.09$ ,  $[\text{S}] = 0.5 \pm 0.2 \text{ }\mu\text{M}$ ; Supplementary Data Table 2) was used to make a background correction for the Tambora samples. This average excludes the background sample for Katmai deposited in 1912, which likely has significant anthropogenic sulfate, supported by its higher concentration and lower isotopic value. The standard deviation of these background samples was used to calculate the final uncertainty on the background-corrected volcanic sulfate  $\delta^{34}\text{S}$  and  $\Delta^{33}\text{S}$  values by Monte Carlo simulations.

The background-corrected volcanic sulfate  $\Delta^{33}\text{S}$  values for the Samalas and Tambora eruptions have a similar positive to negative temporal evolution as the non-background corrected values, but with a larger range (Fig 2). In Tunu2013, the volcanic sulfate  $\Delta^{33}\text{S}$  values for Samalas and Tambora range from 2.8 to -2.5‰ and from 2.2 to -0.85‰, respectively. The volcanic sulfate  $\delta^{34}\text{S}$  values for Samalas and Tambora range from 29.7 to -31.1‰ and 23.4 to -7.9‰, respectively. In contrast, the background-corrected volcanic sulfate for the Katmai eruption in Tunu2013 has  $\delta^{34}\text{S}$  values between 4.4 and -4.3‰ and  $\Delta^{33}\text{S}$  values between 0.3 and 0.6‰, with a different temporal trend (Fig 3). In B40, the Antarctic core, the volcanic sulfate  $\Delta^{33}\text{S}$  and  $\delta^{34}\text{S}$  values for Samalas is very similar to that found in Greenland in Tunu2013, with a range from 1.7 to -2.2‰ and from 19.2 to -24.2‰, respectively (Supplementary Data Table 1).

## 4 Discussion

### 4.1 $\Delta^{33}\text{S}$ constraints on eruptive plume height

The presence of non-zero  $\Delta^{33}\text{S}$  in each of these eruptions implies that some of the  $\text{SO}_2$  from the eruptive plume reached a height in the stratosphere at least as high as the ozone layer (Fig 1). At these altitudes in the atmosphere the  $\text{SO}_2$  was exposed to UV radiation imparting a MIF signal, and this signal was preserved in the sulfate deposited on the ice sheet. For the two tropical eruptions (Tambora and Samalas), this puts a rough constraint of  $> 20\text{km}$  for the eruptive plume. This height constraint is consistent with estimates of the Tambora and Samalas column height of up to  $43\text{ km}$  (Sigurdsson and Carey, 1989; Vidal et al., 2016), which would mean that the  $\text{SO}_2$  was transported well above the ozone layer.

For the extra-tropical Katmai eruption ( $58^\circ\text{ N}$ ), the presence of non-zero  $\Delta^{33}\text{S}$  puts a height constraint of  $>15\text{ km}$  for the eruptive plume, consistent with estimates of a column height of  $17\text{-}26\text{ km}$  for this eruption (Fierstein and Hildreth, 1992). Previous studies (e.g. Schmidt et al., 2012) have questioned whether MIF signals from high latitude eruptions (i.e. proximal to ice sheets) could be preserved in ice, given that a substantial amount of sulfate would be transported directly to the ice sheet via the troposphere or lower stratosphere below the ozone layer with  $\Delta^{33}\text{S} = 0\text{‰}$ . It was hypothesized that this upper tropospheric/lower stratospheric (UT/LS) transport may overwhelm the signal of any MIF from sulfate from at or above the ozone layer. However, our results suggest that the MIF signature can be preserved in ice for high latitude eruptions, albeit more muted (maximum  $\Delta^{33}\text{S}$  values of  $\sim 0.5\text{‰}$ ) than in tropical eruptions (maximum  $\Delta^{33}\text{S}$  values of  $\sim 2\text{‰}$ ) where none of the sulfate was delivered to the ice sheets directly via the troposphere. Thus, the presence of non-zero  $\Delta^{33}\text{S}$  in volcanic sulfate in ice cores provides a minimum height of the eruptive plume

into the stratosphere above the ozone layer, even if the volcano was from the high latitudes. This minimum height will be useful in characterizing the climatic forcing of unknown eruptions because volcanic aerosols that make it to higher altitudes in the stratosphere have a longer residence time, and thus a greater negative radiative forcing, than aerosols that remain in the troposphere (or in the lower levels of the stratosphere below the ozone layer) (Toohey et al., 2019).

## **4.2 Time evolving signature of $\Delta^{33}\text{S}$ and $\delta^{34}\text{S}$ and fingerprinting of tropical and extratropical eruptions**

For all three eruptions, the  $\Delta^{33}\text{S}$  follows a time evolving signature where the initial sulfate deposited has a positive  $\Delta^{33}\text{S}$ , and the later sulfate has a negative  $\Delta^{33}\text{S}$  (Fig 2). This time evolution has been observed before (Baroni et al., 2007) from measurements of sulfate from the 1991 eruption of Pinatubo (Philippines) and the 1963 eruption of Agung (Indonesia) collected from snow pits in Antarctica, and more recently from combined multiple ice cores (Gautier et al., 2018). The initial fractionation process generates a positive  $\Delta^{33}\text{S}$ , and the following negative  $\Delta^{33}\text{S}$  is a result of mass balance (Baroni et al., 2007), with the  $\Delta^{33}\text{S}$  excursion evolving over a timescale of about 3 to 4 years (Fig 2). Given that the timescale over which sulfur dioxide is oxidized to sulfate in the atmosphere is approximately a month, in order to generate the observed isotopic signature that is deposited in the ice over the course of several years there needs to be a spatial separation of these sulfur pools with a differing  $\Delta^{33}\text{S}$  signature (Gautier et al., 2018).

293 We can use the timing and the shape of the  $\Delta^{33}\text{S}$  and  $\delta^{34}\text{S}$  signatures to  
294 fingerprint whether the sulfate from a volcanic event in an ice core was purely  
295 stratospheric (and thus likely tropical) or if some of the sulfate was transported  
296 to the ice sheet via the troposphere (or lower stratosphere below the ozone  
297 layer), and thus likely came from an extra-tropical eruption in the hemisphere of  
298 the ice sheet. In the case of the two tropical eruptions (Fig 2), the peak in the  
299  $\Delta^{33}\text{S}$  comes at the very start of the sulfate deposition; this was also observed in  
300 the case of the Pinatubo and Agung eruptions (Baroni et al., 2007). In contrast,  
301 for the Katmai eruption (Fig 3), the initial sulfate deposited to the ice sheet has a  
302  $\Delta^{33}\text{S} = 0\text{‰}$  because in the case of this high latitude eruption the first sulfate to  
303 arrive to the ice sheet was transported via the troposphere (or lower  
304 stratosphere below the ozone layer) and thus was not fractionated.

305 The  $\delta^{34}\text{S}$  of the tropical eruptions show a strong positive correlation  
306 between the  $\Delta^{33}\text{S}$  and the  $\delta^{34}\text{S}$  ( $r^2 > 0.99$ ; Fig 5); the initial sulfate  $\delta^{34}\text{S}$  increases  
307 and then decreases over the same timeframe as the  $\Delta^{33}\text{S}$  changes. The strong  
308 correlation is because the same process that causes the non-zero  $\Delta^{33}\text{S}$   
309 fractionation in the stratosphere also drives fractionation observed in  $\delta^{34}\text{S}$ , and  
310 since the sulfate in these peaks from tropical eruptions is derived purely from  
311 the stratosphere, this signature is preserved. In contrast, for the Katmai eruption,  
312 the initial volcanic sulfate decreases the  $\delta^{34}\text{S}$  values compared to background  
313  $\delta^{34}\text{S}$  values. This feature can be understood by mass balance: background sulfate  
314 is around  $10\text{‰}$  as it is a mixture of marine ( $21\text{‰}$ ) and volcanic emissions  
315 ( $\sim 0\text{‰}$ ), and thus the addition of more volcanic sulfate with low  $\delta^{34}\text{S}$  (that has  
316 not been fractionated by stratospheric processes as in the case of the tropical

eruptions) would act to decrease the  $\delta^{34}\text{S}$ . This is the opposite of what is measured in the initial  $\delta^{34}\text{S}$  in the tropical eruptions and thus can provide an additional means of distinguishing between unknown tropical and extra-tropical events recorded in ice cores. In contrast to the tropical eruptions, the correlation between  $\delta^{34}\text{S}$  and  $\Delta^{33}\text{S}$  in the sulfate from the Katmai eruption is weak ( $r^2 = 0.37$ ) and negative (slope is -0.05).

Distinguishing between tropical and extra-tropical eruptions in the ice core record of volcanism is important for improving the volcanic radiative forcing record for two reasons. Firstly, constraining the latitudinal band of eruptions has implications for transport and residence time of climatically important aerosols. Secondly, if a fraction of the sulfate deposited in the ice core was delivered through the troposphere, then the associated radiative forcing for that event should be adjusted, as current reconstructions assume that all sulfate deposited in the ice reached the stratosphere (e.g. Toohey and Sigl, 2017). High-resolution sulfur isotope measurements in ice cores thus can potentially provide an additional means of distinguishing between unknown tropical and extra-tropical events recorded in ice cores if this observation is corroborated by further studies.

#### **4.3 Agreement of isotope records between hemispheres**

There is good agreement between the two  $\Delta^{33}\text{S}$  records from Greenland (Tunu2013) and Antarctica (B40) for the Samalas eruption (Fig 4). This agreement suggests that the isotopic signature is primary and is not significantly affected or altered by transport or depositional processes. Furthermore, all three records of tropical eruptions (Tambora from Tunu2013, and Samalas from

Tunu2013 and B40) plot along the same line in  $\Delta^{33}\text{S}$  versus  $\delta^{34}\text{S}$  space within uncertainty (Fig 5; Table 1). The slope of this line is  $0.089 \pm 0.003$  and is the same as the slope of the line derived from eight eruptions from Antarctic ice ( $0.09 \pm 0.02$ ) (Gautier et al., 2018), but is more precisely constrained. When plotted in  $\ln(\delta^{33}\text{S} + 1)$  versus  $\ln(\delta^{34}\text{S} + 1)$  space, the slope of the line is  $0.608 \pm 0.006$ , significantly different from the terrestrial mass dependent slope of 0.515. Thus, the relationship between  $\delta^{33}\text{S}$  and  $\delta^{34}\text{S}$  for volcanic sulfate derived from the stratosphere is predictable and does not appear to differ between ice cores or eruptions. Differences in aerosol transport or deposition, or indeed the timing, hemisphere, or magnitude of the eruption, therefore do not appear to significantly affect the fractionation process (Gautier et al., 2018). This predictable relationship between  $\delta^{33}\text{S}$  and  $\delta^{34}\text{S}$  for volcanic sulfate derived from the stratosphere proves useful in estimating the proportion of stratospheric sulfate from extra-tropical eruptions (see section 4.4).

It remains an open question as to what exact process causes this sulfur isotope fractionation. Gautier et al.(2018) use both  $\Delta^{33}\text{S}$  and  $\Delta^{36}\text{S}$  data from ice cores to estimate the proportion of different oxidation pathways that could explain the isotopic trends. While their data cannot rule out or unambiguously confirm an oxidation pathway, they show that mass independent oxidation pathways (e.g. photolysis or photoexcitation) could account for at least 21% and as much as 91% of the oxidation. Furthermore, they argue that the small variations in the slope in  $\Delta^{33}\text{S}$  versus  $\delta^{34}\text{S}$  space (further confirmed in this study) imply that the relative contribution of different oxidation pathways is similar across eruptions. If the oxidation pathways are similar across different eruptions, then the differences in the magnitude of the mass independent

fractionation between eruptions need to be explained by another process. A recent study (Lin et al., 2018) that considered the correlation between cosmogenic  $^{35}\text{S}$  and  $\Delta^{33}\text{S}$  in modern aerosols proposed that the  $\Delta^{33}\text{S}$  signature is altitude dependent, with greater fractionation occurring higher in the stratosphere. If true, this would prove a useful metric for estimating eruptive plume height in past eruptions, and improving the record of the volcanic forcing of climate.

#### 4.4 Proportion of stratospheric sulfate from Katmai

We can use the high-resolution isotope record from the Katmai eruption and isotope mass balance to calculate the proportion of sulfate that was deposited in the Greenland ice core via the stratosphere. This calculation will improve volcanic forcing indices since these indices typically make the assumption that all of the sulfate deposited on the ice sheets was stratospheric (Toohey and Sigl, 2017), which is likely incorrect in the case of high latitude eruptions such as Katmai. This calculation is based on the following two isotope mass balance equations:

$$\delta^{34}\text{S}_{\text{meas}} = \delta^{34}\text{S}_{\text{strat}} f_{\text{strat}} + \delta^{34}\text{S}_{\text{trop}} (1 - f_{\text{strat}}) \quad (\text{Equation 3})$$

$$\delta^{33}\text{S}_{\text{meas}} = \delta^{33}\text{S}_{\text{strat}} f_{\text{strat}} + \delta^{33}\text{S}_{\text{trop}} (1 - f_{\text{strat}}) \quad (\text{Equation 4})$$

where the subscript *meas* refers to measured isotopic values,  $f_{\text{strat}}$  refers to the fraction of sulfate deposited that came from the stratosphere, and the subscripts *strat* and *trop* refer to the isotopic composition of the sulfate coming from the stratosphere and troposphere respectively. Since sulfate formed in the



troposphere (and lower stratosphere below the ozone layer) follows terrestrial mass dependent fractionation, we can use the following relationship:

$$\delta^{33}\text{S}_{\text{trop}} = \left( (\delta^{34}\text{S}_{\text{trop}} + 1)^{0.515} - 1 \right) \quad (\text{Equation 5})$$

to reduce the number of unknowns in those paired equations. We can further reduce the number of unknowns since the stratospheric sulfate measured in ice cores follows the following relationship (see Section 4.3):

$$\delta^{33}\text{S}_{\text{strat}} = ((\delta^{34}\text{S}_{\text{strat}} + 1)^{0.608} - 1) \quad (\text{Equation 6})$$

with an uncertainty on the exponent  $\lambda = 0.608$  of 0.006. Combining equations 3 to 6 gives two equations with three unknowns:  $\delta^{34}\text{S}_{\text{strat}}$ ,  $\delta^{34}\text{S}_{\text{trop}}$ , and  $f_{\text{strat}}$ . Thus if we make an assumption of the isotopic composition of the volcanic  $\delta^{34}\text{S}_{\text{trop}}$ , we can solve for  $f_{\text{strat}}$  and  $\delta^{34}\text{S}_{\text{strat}}$ . The sulfur isotopic composition of volcanic  $\text{SO}_2$  can vary significantly away from a mantle value (0‰, V-CDT) as a function of the mantle source and the oxygen fugacity of the magma (e.g. de Moor et al., 2010; Mather et al., 2006). To address this, we calculate the  $f_{\text{strat}}$  and corresponding uncertainty using a 500 iteration Monte Carlo simulation for a uniformly distributed range of  $\delta^{34}\text{S}_{\text{trop}}$  values from -10 to 10‰. The uncertainties on the measured values and exponent  $\lambda$  are assumed to be normally distributed. We find that the  $f_{\text{strat}}$  values for the Katmai samples range from 0.26 to 0.88, and that when integrated over the whole peak, the proportion of the sulfate peak that came from the stratosphere was 0.55, with an uncertainty range of 0.35 to 0.62. Constraints on the  $\delta^{34}\text{S}_{\text{trop}}$  for this specific eruption would help to narrow the range of uncertainty of the fraction of stratospheric sulfate deposited in Greenland. Even so, this estimate improves upon the assumption that all of the sulfate deposited came from the stratosphere (Toohey and Sigl, 2017). It also

helps to reconcile estimates of stratospheric sulfate loading from studies using pyrhelimetric optical depth perturbations with estimates based purely on the sulfate deposition in Greenland, which are greater than the optical depth estimates by a factor of three (11 Tg compared to 30 Tg (Hammer et al., 1980; Stothers, 1996)). This approach may thus be used in future studies to improve volcanic forcing indices.

## 5. Conclusion

Sulfur isotopes of volcanic sulfate deposited in ice cores can be used to identify if the sulfate came from above the ozone layer in the stratosphere, since exposure to UV radiation imparts a mass independent fractionation, recorded as a non-zero  $\Delta^{33}\text{S}$  (Savarino et al., 2003). There is good agreement between isotope records from Greenland and Antarctica over the same volcanic event, indicating that sulfur isotopes are not significantly affected by transportation or depositional processes. Our method of analysis by MC-ICPMS requires only 10 nmol of sulfur, allowing for up to bi-monthly resolution over the volcanic sulfate peak in the ice cores from samples as small as 4 mL. These high-resolution records show distinct differences between tropical (Samalas and Tambora) and extra-tropical (Katmai) eruptions. In the case of the tropical eruptions, all of the sulfate deposited on the ice sheet came via the stratosphere, and thus the  $\delta^{34}\text{S}$  and  $\Delta^{33}\text{S}$  values are strongly correlated, with the initial sulfate deposited showing an increase in both values. In contrast, for the extra-tropical eruption, some of the sulfate was deposited in Greenland via the troposphere or lower stratosphere below the ozone layer, and thus the initial signal of the volcanic

sulfate is a decrease in its  $\delta^{34}\text{S}$  value, with  $\Delta^{33}\text{S}$  values within error of zero. Isotope mass balance on extra-tropical eruptions such as Katmai can be used to estimate the proportion of the volcanic sulfate deposited in the ice core that came via the stratosphere. These measurements will help to improve the record of the volcanic forcing of climate for unidentified eruptions in the past, which should in turn improve simulations of historical climate change.

## Acknowledgements

This research was funded by a Foster and Coco Stanback postdoctoral fellowship and a Marie Curie Career Integration Grant (CIG14-631752) to AB and a NSF-OCE grant 1340174 and NSF-EAR grant 1349858 to JFA. MS acknowledges funding from the European Research Council (ERC) under the European Union's Horizon 2020 research and innovation programme (grant agreement No 820047) NSF-PLR grant 1204176 to JRM supported collection and analysis of the Tunu2013 core. We thank Sepp Kipfstuhl of the Alfred Wegener Institut for providing the B40 core. We thank Joel Savarino, an anonymous reviewer, and James Rae for comments on this manuscript.

## References

- Baroni, M., Savarino, J., Cole-Dai, J., Rai, V.K., Thiemens, M.H., 2008. Anomalous sulfur isotope compositions of volcanic sulfate over the last millennium in Antarctic ice cores. *Journal of Geophysical Research* 113, D20112. doi:10.1029/2008JD010185
- Baroni, M., Thiemens, M.H., Delmas, R.J., Savarino, J., 2007. Mass-Independent Sulfur Isotopic Compositions in Stratospheric Volcanic Eruptions. *Science* 315, 84–87. doi:10.1126/science.1131754
- Burke, A., Present, T.M., Paris, G., Rae, E.C.M., Sandilands, B.H., Gaillardet, J., Peucker-Ehrenbrink, B., Fischer, W.W., McClelland, J.W., Spencer, R.G.M., Voss, B.M., Adkins, J.F., 2018. Sulfur isotopes in rivers: Insights into global weathering budgets, pyrite oxidation, and the modern sulfur cycle. *Earth and Planetary Science Letters* 496, 168–177. doi:10.1016/j.epsl.2018.05.022
- Cole-Dai, J., Ferris, D., Lanciki, A., Savarino, J., Baroni, M., Thiemens, M.H., 2009.

- Cold decade (AD 1810–1819) caused by Tambora (1815) and another (1809) stratospheric volcanic eruption. *Geophys. Res. Lett.* 36. doi:10.1029/2009GL040882
- de Moor, J.M., Fischer, T.P., Sharp, Z.D., Hauri, E.H., Hilton, D.R., Atudorei, V., 2010. Sulfur isotope fractionation during the May 2003 eruption of Anatahan volcano, Mariana Islands: Implications for sulfur sources and plume processes. *Geochimica et Cosmochimica Acta* 74, 5382–5397. doi:10.1016/j.gca.2010.06.027
- Farquhar, J., Savarino, J., Airieau, S., and Thiemens, M. H., 2001. Observation of wavelength-sensitive mass-independent sulfur isotope effects during SO<sub>2</sub> photolysis: Application to the early atmosphere, *J. Geophys. Res.*, 106, 32829–32840, 10.1029/2000JE001437.
- Fierstein, J., Hildreth, W., 1992. The Plinian Eruptions of 1912 at Novarupta, Katmai-National-Park, Alaska. *Bull Volcanol* 54, 646–684. doi:10.1007/BF00430778
- Gao, C., Oman, L., Robock, A., Stenchikov, G.L., 2007. Atmospheric volcanic loading derived from bipolar ice cores: Accounting for the spatial distribution of volcanic deposition. *Journal of Geophysical Research* 112, D09109. doi:10.1029/2006JD007461
- Gao, C., Robock, A., Ammann, C., 2008. Volcanic forcing of climate over the past 1500 years: An improved ice core-based index for climate models. *Journal of Geophysical Research* 113, D23111. doi:10.1029/2008JD010239
- Gautier, E., Savarino, J., Erbland, J., Farquhar, J., 2018. SO<sub>2</sub> Oxidation Kinetics Leave a Consistent Isotopic Imprint on Volcanic Ice Core Sulfate. *J. Geophys. Res. Atmos.* 117, D06216–12. doi:10.1029/2018JD028456
- Gautier, E., Savarino, J., Hoek, J., Erbland, J., Caillon, N., Hattori, S., Yoshida, N., Albalat, E., Albarede, F., Farquhar, J., 2019. 2600-years of stratospheric volcanism through sulfate isotopes. *Nature Communications* 10, 1–7. doi:10.1038/s41467-019-08357-0
- Hammer, C.U., Clausen, H.B., Dansgaard, W., 1980. Greenland ice sheet evidence of post-glacial volcanism and its climatic impact. *Nature Publishing Group* 288, 230–235. doi:10.1038/288230a0
- Lanciki, A., Cole-Dai, J., Thiemens, M.H., Savarino, J., 2012. Sulfur isotope evidence of little or no stratospheric impact by the 1783 Laki volcanic eruption. *Geophys. Res. Lett.* 39, n/a–n/a. doi:10.1029/2011GL050075
- Lin, M., Zhang, X., Li, M., Xu, Y., Zhang, Z., Tao, J., Su, B., Liu, L., Shen, Y., Thiemens, M.H., 2018. Five-S-isotope evidence of two distinct mass-independent sulfur isotope effects and implications for the modern and Archean atmospheres. *Proceedings of the National Academy of Sciences* 115, 8541–8546. doi:10.1073/pnas.1803420115
- Mather, T.A., McCabe, J.R., Rai, V.K., Thiemens, M.H., Pyle, D.M., Heaton, T.H.E., Sloane, H.J., Fern, G.R., 2006. Oxygen and sulfur isotopic composition of volcanic sulfate aerosol at the point of emission. *Journal of Geophysical Research* 111, 1685–9. doi:10.1029/2005JD006584
- McConnell, J.R., Burke, A., Dunbar, N.W., Kohler, P., Thomas, J.L., Arienzo, M.M., Chellman, N.J., Maselli, O.J., Sigl, M., Adkins, J.F., Baggenstos, D., Burkhardt, J.F., Brook, E.J., Buizert, C., Cole-Dai, J., Fudge, T.J., Knorr, G., Graf, H.-F., Grieman, M.M., Iverson, N., McGwire, K.C., Mulvaney, R., Paris, G., Rhodes, R.H., Saltzman, E.S., Severinghaus, J.P., Steffensen, J.P., Taylor, K.C., Winckler, G.,

2017. Synchronous volcanic eruptions and abrupt climate change ~17.7 ka plausibly linked by stratospheric ozone depletion. *Proceedings of the National Academy of Sciences* 114, 10035–10040. doi:10.1073/pnas.1705595114
- McConnell, J.R., Wilson, A.I., Stohl, A., Arienzo, M.M., Chellman, N.J., Eckhardt, S., Thompson, E.M., Pollard, A.M., Steffensen, J.P., 2018. Lead pollution recorded in Greenland ice indicates European emissions tracked plagues, wars, and imperial expansion during antiquity. *Proceedings of the National Academy of Sciences* 115, 5726–5731. doi:10.1073/pnas.1721818115
- Paris, G., Sessions, A.L., Subhas, A.V., Adkins, J.F., 2013. MC-ICP-MS measurement of  $\delta^{34}\text{S}$  and  $\Delta^{33}\text{S}$  in small amounts of dissolved sulfate. *Chemical Geology* 345, 50–61. doi:10.1016/j.chemgeo.2013.02.022
- Plummer, C.T., Curran, M.A.J., van Ommen, T.D., Rasmussen, S.O., Moy, A.D., Vance, T.R., Clausen, H.B., Vinther, B.M., Mayewski, P.A., 2012. An independently dated 2000-yr volcanic record from Law Dome, East Antarctica, including a new perspective on the dating of the 1450s CE eruption of Kuwae, Vanuatu. *Clim. Past* 8, 1929–1940. doi:10.5194/cp-8-1929-2012
- Robock, A., 2000. Volcanic eruptions and climate. *Rev. Geophys.* 38, 191–219. doi:10.1029/1998RG000054
- Savarino, J., 2003. UV induced mass-independent sulfur isotope fractionation in stratospheric volcanic sulfate. *Geophys. Res. Lett.* 30, 2131. doi:10.1029/2003GL018134
- Schmidt, A., Thordarson, T., Oman, L.D., Robock, A., Self, S., 2012. Climatic impact of the long-lasting 1783 Laki eruption: Inapplicability of mass-independent sulfur isotopic composition measurements. *Journal of Geophysical Research* 117, n/a–n/a. doi:10.1029/2012JD018414
- Schurer, A.P., 2013. Small influence of solar variability on climate over the past millennium. *Nature Geoscience* 7, 1–5. doi:10.1038/ngeo2040
- Sigl, M., McConnell, J.R., Layman, L., Maselli, O., McGwire, K., Pasteris, D., Dahl-Jensen, D., Steffensen, J.P., Vinther, B., Edwards, R., Mulvaney, R., Kipfstuhl, S., 2013. A new bipolar ice core record of volcanism from WAIS Divide and NEEM and implications for climate forcing of the last 2000 years. *J. Geophys. Res. Atmos.* 118, 1151–1169. doi:10.1029/2012JD018603
- Sigl, M., McConnell, J.R., Toohey, M., Curran, M., Das, S.B., Edwards, R., Isaksson, E., Kawamura, K., Kipfstuhl, S., Krüger, K., Layman, L., Maselli, O.J., Motizuki, Y., Motoyama, H., Pasteris, D.R., Severi, M., 2014. Insights from Antarctica on volcanic forcing during the Common Era. *Nature Clim Change* 4, 693–697. doi:10.1038/nclimate2293
- Sigl, M., Winstrup, M., McConnell, J.R., Welten, K.C., Plunkett, G., Ludlow, F., Büntgen, U., Caffee, M., Chellman, N., Dahl-Jensen, D., Fischer, H., Kipfstuhl, S., Kostick, C., Maselli, O.J., Mekhaldi, F., Mulvaney, R., Muscheler, R., Pasteris, D.R., Pilcher, J.R., Salzer, M., Schüpbach, S., Steffensen, J.P., Vinther, B.M., Woodruff, T.E., 2015. Timing and climate forcing of volcanic eruptions for the past 2,500 years. *Nature* 523, 543–549. doi:10.1038/nature14565
- Sigurdsson, H., Carey, S., 1989. Plinian and co-ignimbrite tephra fall from the 1815 eruption of Tambora volcano. *Bull Volcanol* 51, 243–270. doi:10.1007/BF01073515
- Stothers, R.B., 1996. Major optical depth perturbations to the stratosphere from

volcanic eruptions: Pyrheliometric period, 1881–1960. *J. Geophys. Res. Atmos.* doi:10.1029/95JD03237/pdf

Toohey, M., Ger, K.K.X., Schmidt, H., Timmreck, C., Sigl, M., Stoffel, M., Wilson, R., 2019. Disproportionately strong climate forcing from extratropical explosive volcanic eruptions. *Nature Geoscience* 12, 1–10. doi:10.1038/s41561-018-0286-2

Toohey, M., Sigl, M., 2017. Volcanic stratospheric sulfur injections and aerosol optical depth from 500 BCE to 1900 CE. *earth-syst-sci-data.net* 9, 809–831. doi:10.1594/WDCC/eVolv2k\_v2

Vidal, C.M., Métrich, N., Komorowski, J.-C., Pratomo, I., Michel, A., Kartadinata, N., Robert, V., Lavigne, F., 2016. The 1257 Samalas eruption (Lombok, Indonesia): the single greatest stratospheric gas release of the Common Era. *Sci. Rep.* 6, 1–13. doi:10.1038/srep34868

## Figures

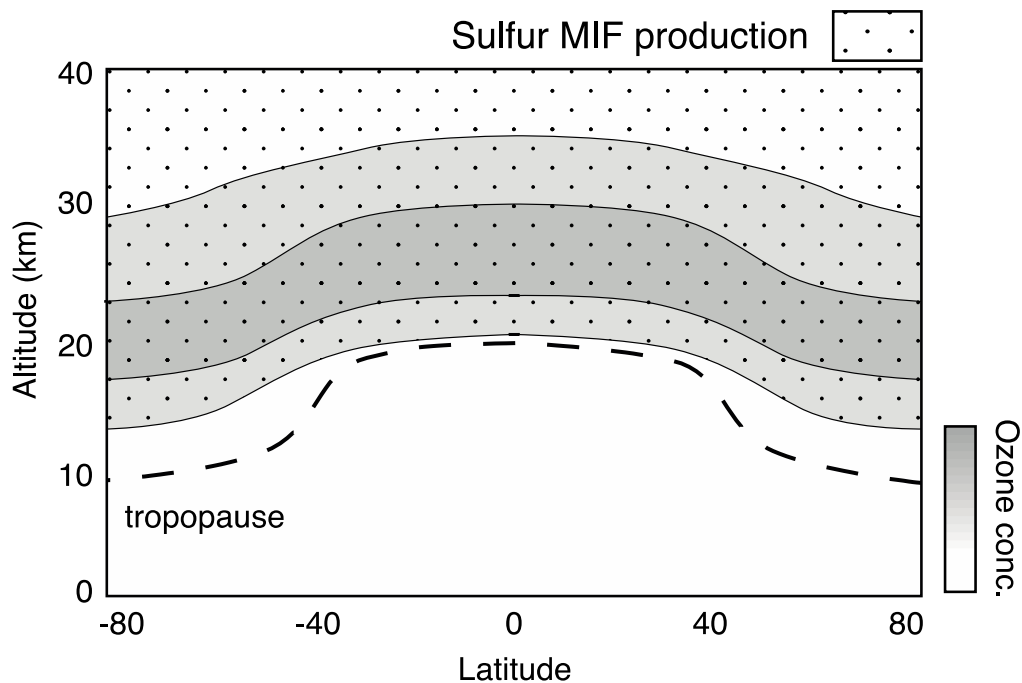


**Fig 1.** Schematic of sulfur mass independent fractionation (MIF) production. The formation of sulfur MIF requires UV radiation, and therefore it is limited to altitudes in the stratosphere at or above the ozone layer (indicated on schematic by stippling). Without knowing the exact mechanism of sulfur MIF formation it is not currently possible to put more precise altitude constraints on the process. At high latitudes there is a region of the stratosphere that lies below the ozone layer where MIF is not produced. Thus the presence of MIF in polar ice provides a means to identify eruptions whose plumes reached high altitudes in the stratosphere; high latitude eruptions into the lower stratosphere would not produce sulfur MIF.

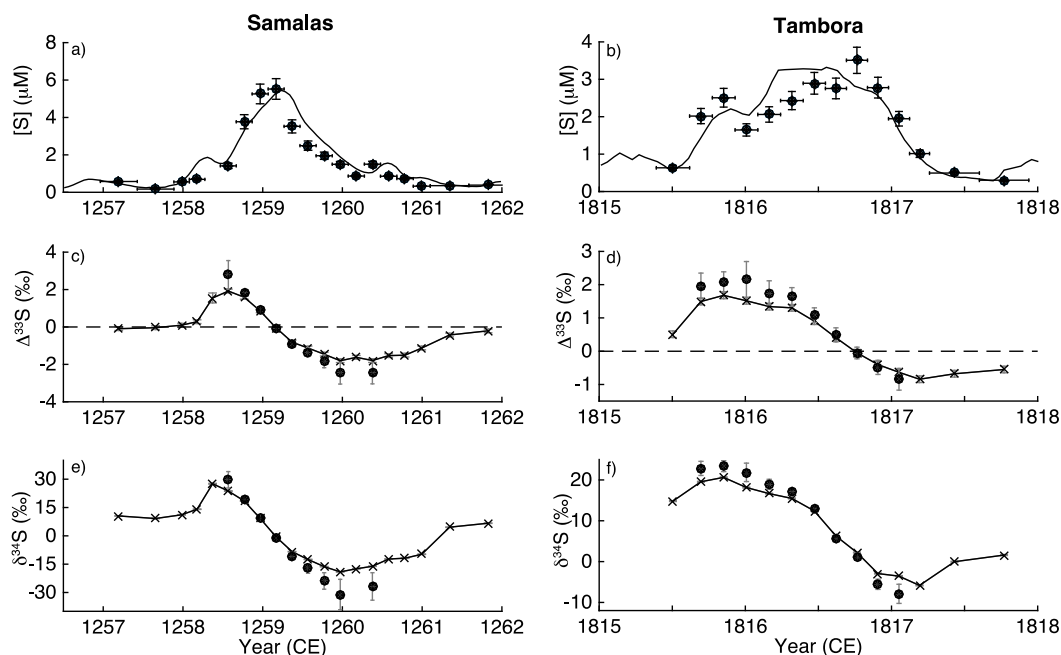
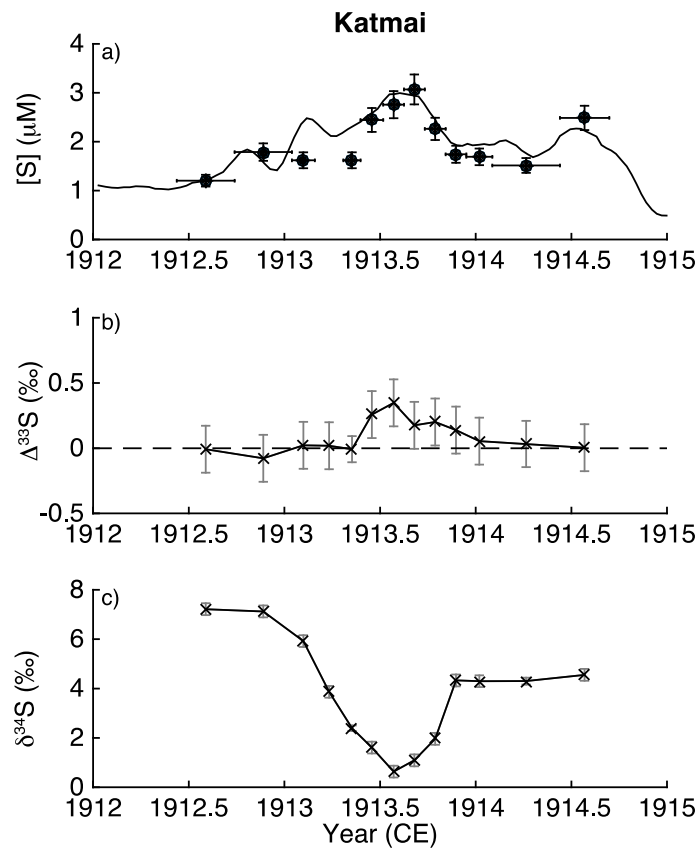


**Fig 2.** Sulfur concentration (a, b) and isotope curves (c-f) versus time for two tropical eruptions recorded in Tunu2013 ice core in Greenland: the 1258 eruption of Samalas (a,c,f) and the 1815 eruption of Tambora (b,d,e). The line in (a,b) is the continuous melting sulfur concentration from (Sigl et al., 2015) and it is compared to sulfur concentration measurements by ion chromatograph on the discrete samples that were subsequently measured for isotopes (circles). (c,d)  $\Delta^{33}\text{S}$  (‰) measured in the ice samples (x's) and the background corrected volcanic  $\Delta^{33}\text{S}$  (circles) for samples with more than 65% volcanic sulfate (see text). (e,f) is the same as (c,d), but for  $\delta^{34}\text{S}$  (‰, V-CDT).





606

607 **Fig 3.** Sulfur concentration (a),  $\Delta^{33}\text{S}$  (b), and  $\delta^{34}\text{S}$  (c) versus time for the high  
 608 latitude eruption Katmai/Novarupta in 1912. The symbols are the same as in  
 609 Figure 2.

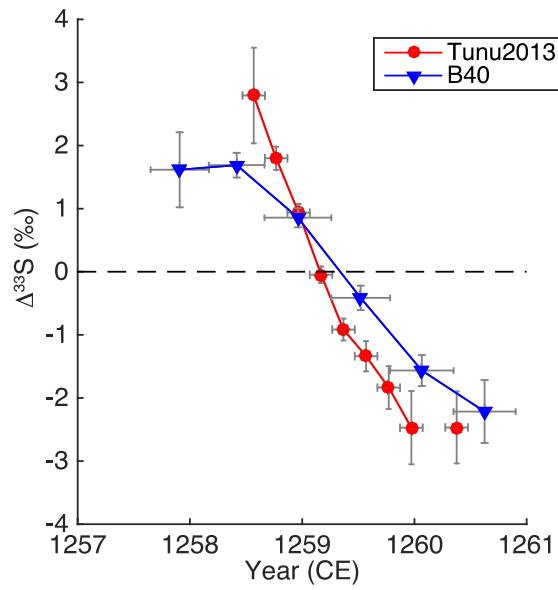


**Fig 4.** Background-corrected volcanic  $\Delta^{33}\text{S}$  (‰) across the Samalas volcanic event from the Tunu2013 ice core (Greenland, red circles) and the B40 ice core (Antarctica, blue triangles).

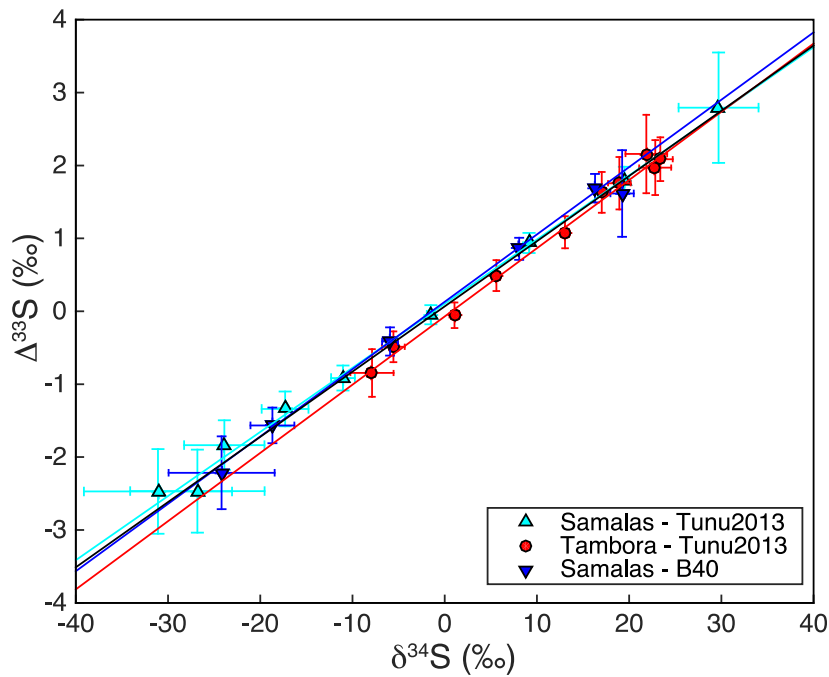


**Fig 5.** Cross plot of  $\Delta^{33}\text{S}$  versus  $\delta^{34}\text{S}$  for the background-corrected volcanic sulfate from tropical eruptions Tambora (red circles) and Samalas (cyan upward triangle measured in Tunu2013, blue downward triangle measured in B40). Regression lines are plotted in the color of the symbols. Black line is the regression considering all of the data. The size of the error bars is driven by uncertainty in the background correction, as analytical uncertainties are  $\sim 0.1\text{‰}$  for both  $\Delta^{33}\text{S}$  and  $\delta^{34}\text{S}$ .

**Table 1. Regression solution parameters.** Slope and intercept values for linear regressions of  $\Delta^{33}\text{S}$  versus  $\delta^{34}\text{S}$  data and  $\ln(\delta^{33}\text{S}+1)$  versus  $\ln(\delta^{34}\text{S}+1)$  data for each individual tropical eruption and for all data combined. Uncertainties encompass the 95% confidence interval.

Eruption	Core	$\Delta^{33}\text{S}$ versus $\delta^{34}\text{S}$		$\ln(\delta^{33}\text{S}+1)$ versus $\ln(\delta^{34}\text{S}+1)$	
		slope	intercept	slope	intercept
Samalas	Tunu2013	$0.088 \pm 0.003$	$0.10 \pm 0.03$	$0.604 \pm 0.003$	$0.1 \pm 0.05$
Samalas	B40	$0.092 \pm 0.007$	$0.13 \pm 0.04$	$0.610 \pm 0.006$	$0.1 \pm 0.1$
Tambora	Tunu2013	$0.094 \pm 0.005$	$-0.07 \pm 0.08$	$0.609 \pm 0.006$	$-0.08 \pm 0.07$
<b>All data</b>		<b><math>0.089 \pm 0.003</math></b>	<b><math>0.07 \pm 0.05</math></b>	<b><math>0.608 \pm 0.006</math></b>	<b><math>0.06 \pm 0.07</math></b>